

## Porphyrin and Tetrabenzoporphyrin Dendrimers: Tunable Membrane-Impermeable Fluorescent pH Nanosensors

Olga Finikova,<sup>†</sup> Alexander Galkin,<sup>‡</sup> Vladimir Rozhkov,<sup>†</sup> Maria Cordero,<sup>†</sup>  
Cecilia Hägerhäll,<sup>‡</sup> and Sergei Vinogradov<sup>\*†</sup>

Contribution from the Department of Biochemistry and Biophysics, University of Pennsylvania, Philadelphia, Pennsylvania 19104, and Department of Biochemistry, University of Lund, Lund, Sweden

Received January 14, 2003; E-mail: vinograd@mail.med.upenn.edu

**Abstract:** The pH dependencies of the UV–vis and fluorescent spectra of new water-soluble dendritic porphyrins and tetrabenzoporphyrins were studied. Because of extended  $\pi$ -conjugation and nonplanar distortion, the absorption and the emission bands of tetraaryl-tetrabenzoporphyrins ( $Ar_4TBP$ ) are red-shifted and do not overlap with those of regular tetraarylporphyrins ( $Ar_4P$ ). When encapsulated inside dendrimers with hydrophilic outer layers,  $Ar_4Ps$  and  $Ar_4TBPs$  become water soluble and can serve as pH indicators, with  $pK$ 's adjustable by the peripheral charges on the dendrimers. Two new dendritic porphyrins, Gen 4 polyglutamic porphyrin dendrimer  $H_2P-Glu^4OH$  (**1**) with 64 peripheral carboxylates and Gen 1 poly(ester amide) Newkome-type tetrabenzoporphyrin dendrimer  $H_2TBP-Nw^1OH$  (**2**) with 36 peripheral carboxylates, were synthesized and characterized. The  $pK$ 's of the encapsulated porphyrins ( $pK_{H_2P-Glu^4OH} = 6.2$  and  $pK_{H_2TBP-Nw^1OH} = 6.3$ ) were found to be strongly influenced by the dendrimers, revealing significant electrostatic shielding of the cores by the peripheral charges. The titration curves obtained by differential excitation using the mixtures of the dendrimers were shown to be identical to those determined for the dendrimers individually. Due to their peripheral carboxylates and nanometric molecular size, porphyrin dendrimers cannot penetrate through phospholipid membranes. Dendrimer **1** was captured inside phospholipid liposomes, which were suspended in a solution containing dendrimer **2**. No response from **1** was detected upon pH changes in the bulk solution, while the response from **2** was predictably strong. When proton channels were created in the liposome walls, both compounds responded equally to the bulk pH changes. These results suggest that porphyrin dendrimers can be used as fluorescent pH indicators for proton gradient measurements.

### Introduction

The past two decades have been marked by rapid progress in dendrimer synthesis.<sup>1</sup> A broad variety of dendrimers has been generated during this time, and as a result, current research has focused primarily on new areas of dendrimer application. In the interest of discovering their practical potential, dendrimers with functional moieties and particularly dendrimers incorporating photo- or electroactive cores have been under extensive scrutiny in recent years.<sup>2</sup> A number of elegant models for energy<sup>3</sup> and electron-transfer studies,<sup>4</sup> light-harvesting systems,<sup>3,5</sup> and catalysts<sup>6</sup> have been created using these compounds, suggesting new ways to utilize the unique structural features of dendrimers.

One especially intriguing class of core-modified dendrimers consists of dendritic porphyrins or porphyrin dendrimers.<sup>7</sup> The initial interest in these molecules stemmed from their resemblance to heme-containing proteins. Porphyrins caged inside dendritic shells are structurally reminiscent of enzymes, in which

<sup>†</sup> University of Pennsylvania.

<sup>‡</sup> University of Lund.

- (1) For selected reviews, see: (a) Fréchet, J. M. J. *Science* **1994**, *263*, 1710. (b) Fischer, M.; Vögtle, F. *Angew. Chem., Int. Ed. Engl.* **1999**, *38*, 885. (c) Grayson, S. K.; Fréchet, J. M. J. *Chem. Rev.* **2001**, *101*, 3819. (d) Tomalia, D. A.; Fréchet, J. M. J. *J. Polym. Sci., A* **2002**, *40*, 2719.
- (2) For selected reviews, see: (a) Smith, D. K.; Diederich, F. *Chem.—Eur. J.* **1998**, *4*, 1353. (b) Gorman, C. B.; Smith, J. C. *Acc. Chem. Res.* **2001**, *34*, 60. (c) Vögtle, F.; Gestermann, S.; Hesse, R.; Schwier, H.; Windisch, B. *Prog. Polym. Sci.* **2000**, *25*, 987. (d) Hecht, S.; Fréchet, J. M. J. *Angew. Chem., Int. Ed.* **2001**, *40*, 74. (e) Dykes, G. M. *J. Chem. Technol. Biotechnol.* **2001**, *76*, 903. (f) Stiriba, S. E.; Frey, H.; Haag, R. *Angew. Chem., Int. Ed.* **2002**, *41*, 1329. (g) Cameron, C. S.; Gorman, C. B. *Adv. Funct. Mater.* **2002**, *12*, 17.

- (3) For examples, see: (a) Stewart, G. M.; Fox, M. A. *J. Am. Chem. Soc.* **1996**, *118*, 4354. (b) Devadoss, C.; Bharathi, P.; Moore, J. S. *J. Am. Chem. Soc.* **1996**, *118*, 9635. (c) Plevoets, M.; Vögtle, F.; De Cola, L.; Balzani, V. *New J. Chem.* **1999**, *23*, 63. (d) Gilat, S. L.; Adronov, A.; Fréchet, J. M. J. *Angew. Chem., Int. Ed.* **1999**, *38*, 1422. (f) Schultze, X.; Serin, J.; Adronov, A.; Fréchet, J. M. J. *Chem. Commun.* **2001**, 1160. (g) Choi, M. S.; Aida, T.; Yamazaki, T.; Yamazaki, I. *Angew. Chem., Int. Ed.* **2001**, *40*, 3194.
- (4) For examples, see: (a) Sadamoto, R.; Nobuyuki, T.; Aida, T. *J. Am. Chem. Soc.* **1996**, *118*, 3978. (b) Gorman, C. B.; Smith, J. C.; Hager, M. W.; Parkhurst, B. L.; Sierzputowska-Gracz, H.; Haney, C. A. *J. Am. Chem. Soc.* **1999**, *121*, 9958. (c) Camps, X.; Diemel, E.; Hirsch, A.; Pyo, S.; Echegoyen, L.; Hackbarth, S.; Roder, R. *Chem.—Eur. J.* **1999**, *5*, 2362. (d) Capostoi, G. J.; Cramer, S. J.; Rajesh, C. S.; Modarelli, D. A. *Org. Lett.* **2001**, *3*, 1645. (e) Rajesh, C. S.; Capostoi, G. J.; Cramer, S. J.; Modarelli, D. A. *J. Phys. Chem. B* **2001**, *105*, 10175. (f) Toba, R.; Quintela, J. M.; Peinador, C.; Roman, E.; Kaifer, A. E. *Chem. Commun.* **2001**, 857. (g) Ghaddar, T. H.; Wishart, J. F.; Thompson, D. W.; Whitesell, J. K.; Fox, M. A. *J. Am. Chem. Soc.* **2002**, *124*, 8285. (g) Lor, M.; Thielemans, J.; Vaele, L.; Cotlet, M.; Hofkens, J.; Weil, T.; Hampel, C.; Mullen, K.; Verhoeven, J. W.; Van der Auweraer, M.; De Schryver, F. C. *J. Am. Chem. Soc.* **2002**, *124*, 9918.
- (5) For examples, see: (a) Bar-Haim, A.; Klafter, J. *J. Lumin.* **1998**, *76*, 197. (b) Adronov, A.; Gilat, S. L.; Fréchet, J. M. J.; Ohta, K.; Neuwahl, F. V. R.; Fleming, G. R. *J. Am. Chem. Soc.* **2000**, *122*, 1175. (c) Balzani, V.; Juris, A. *Coord. Chem. Rev.* **2001**, *211*, 97. (d) Adronov, A.; Robello, D. R.; Fréchet, J. M. J. *J. Polym. Sci., A* **2001**, *39*, 1366.

hydrophobic hemes are buried deep inside the polypeptide superstructures and are protected from direct interactions with solvent and solutes. Mimicking the protein matrix, hydrophobic dendritic wedges in porphyrin dendrimers modulate various thermodynamic properties of the encapsulated cores, e.g. their electrochemical potentials,<sup>7b-e,i</sup> and control the accessibility of the cores to small molecules.<sup>7a,c,f,j</sup> Similar control is offered by dendrimers to other than porphyrin-encapsulated centers.<sup>2b,g,8</sup> The isolation, solubilization, and possibility to modulate the properties of porphyrins via dendritic encapsulation have all been employed in catalysis<sup>6a-c,e,f</sup> and more recently in small molecule sensing.<sup>9</sup>

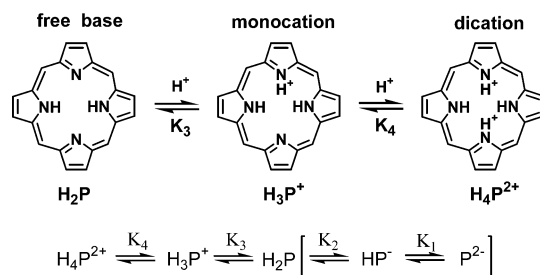
Previously, as part of the studies aiming to design phosphors for in vivo oxygen sensing, we synthesized a series of water-soluble polyglutamic porphyrin dendrimers.<sup>9</sup> In the case of free-base porphyrin dendrimers,<sup>9c</sup> the protonation constants of the cores were shown to change with the size of the attached dendritic ligands, suggesting that the negative charges on the outer layer of dendrimers stabilize the porphyrin dications, possibly via through-space electrostatic shielding. The observed effect revealed an opportunity to use the peripheral charges on dendrimers as a p*K*-tuning tool. At the same time, the encapsulation itself could be used to increase the solubility of porphyrins and to prevent their aggregation in aqueous solutions. Considering the rich spectroscopy of tetrapyrrolic macrocycles and recent advances in the chemistry of near-infrared absorbing extended porphyrins,<sup>10</sup> it became of interest to explore the possibility of using porphyrin dendrimers as colorimetric and/or luminescent pH sensors. Even though many such indicators are available,<sup>11</sup>

porphyrin dendrimers offer a number of advantages over the existing commercial dyes, especially for pH measurements in biological systems. One of these advantages is the complete membrane impermeability of porphyrin dendrimers—an intrinsic structural property of large dendritic spheres carrying multiple peripheral charges. Of a special interest is the possibility of selecting a number of porphyrins with nonoverlapping absorption and emission bands and using them simultaneously for pH-gradient measurements in compartmentalized biological systems. The design of such a pair was, in fact, the driving force behind this study, since the elucidation of proton translocation mechanisms by respiratory chain enzymes has been the long-term interest of some of the authors.<sup>12</sup> In the following paragraphs we attempt to clarify the ideas behind our design by summarizing some relevant information from the porphyrin spectroscopy.

Optical absorption spectra of porphyrins contain a number of bands in the UV–vis and near-infrared regions (Soret and Q-bands). The positions of these bands depend on the exact structures of the porphyrins; however, one general trend is that the absorption maxima shift to the red upon macrocycle distortion<sup>13</sup> and/or upon conjugation of one or more pyrrole rings with external  $\pi$ -systems.<sup>10,14</sup>

Porphyrins are highly fluorescent molecules. Their emission quantum yields are in the range of 10–30%, and their fluorescence can be excited at different locations throughout the visible spectrum. The fluorescence of porphyrins exhibits relatively large Stokes shifts (30–50 nm) and responds to substitution effects in much the same way as does the absorption; i.e., emission bands migrate to the red upon macrocycle distortion and/or  $\pi$ -conjugation. Importantly, distortion also usually diminishes the fluorescence quantum yields of porphyrins—a fact that must be considered when attempting to use these molecules as fluorescent markers.

Two imine nitrogens of a free-base porphyrin (H<sub>2</sub>P) are able to attach protons forming porphyrin mono- (H<sub>3</sub>P<sup>+</sup>) and dications (H<sub>4</sub>P<sup>2+</sup>): Traditionally, constants *K*<sub>3</sub> and *K*<sub>4</sub> are associated with



imine-N protonations, while the constants *K*<sub>1</sub> and *K*<sub>2</sub> correspond to the removal of amine protons and the formation of porphyrin anions.<sup>15</sup> Upon protonation, both the absorption and emission (fluorescence) spectra of porphyrins undergo strong changes, which makes it possible to determine p*K*<sub>3</sub> and p*K*<sub>4</sub> by optical methods. For the majority of porphyrins, constants p*K*<sub>3</sub> and p*K*<sub>4</sub> are close (less than 2 pH units apart). Therefore, their individual

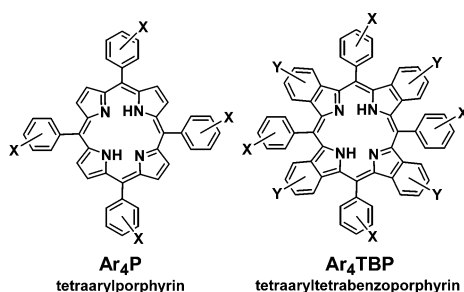
- (6) For examples, see: (a) Bhyrappa, P.; Young, J. K.; Moore, J. S.; Suslick, K. S. *J. Am. Chem. Soc.* **1996**, *118*, 5708. (b) Bhyrappa, P.; Vijayanthimala, G.; Suslick, K. S. *J. Am. Chem. Soc.* **1999**, *121*, 262. (c) Kimura, M.; Shiba, T.; Yamazaki, M.; Hanabusa, K.; Shirai, H.; Kobayashi, N. *J. Am. Chem. Soc.* **2001**, *123*, 5636–5642. (d) Hecht, S.; Fréchet, J. M. J. *J. Am. Chem. Soc.* **2001**, *123*, 6959. (e) Davis, A. V.; Driffield, M.; Smith, D. K. *Org. Lett.* **2001**, *3*, 3075. (f) Uyemura, M.; Aida, T. *J. Am. Chem. Soc.* **2002**, *124*, 11392. (g) Zhang, J. L.; Zhou, H. B.; Huang, J. S.; Che, C. M. *Chem.—Eur. J.* **2002**, *8*, 1554. (h) Twyman, L. J.; King, A. S. H.; Martin, I. K. *Chem. Soc. Rev.* **2002**, *31*, 69 and references therein.
- (7) (a) Jin, R. H.; Aida, T.; Inoue, S. *Chem. Commun.* **1993**, 1260. (b) Dandliker, P. J.; Diederich, F.; Gisselbrecht, J. P.; Louati, A.; Gross, M. *Angew. Chem., Int. Ed. Engl.* **1996**, *34*, 2725. (c) Tomoyose, Y.; Jiang, D. L.; Jin, R. H.; Aida, T.; Yamashita, T.; Horie, K.; Yashima, E.; Okamoto, Y. *Macromolecules* **1996**, *29*, 5236. (d) Collman, J. P.; Fu, L.; Zingg, A.; Diederich, F. *Chem. Commun.* **1997**, 193. (e) Dandliker, P. J.; Diederich, F.; Zingg, A.; Gisselbrecht, J. P.; Gross, M.; Louati, A.; Sanford, E. *Helv. Chim. Acta* **1997**, *80*, 1773. (f) Pollak, K. W.; Sanford, E. M.; Fréchet, J. M. J. *J. Mater. Chem.* **1998**, *8*, 519. (g) Tomioka, N.; Takasu, D.; Takahashi, T.; Aida, T. *Angew. Chem., Int. Ed.* **1998**, *37*, 1531. (h) Weyermann, P.; Diederich, F. *J. Chem. Soc., Perkin Trans. 1* **2000**, 4231. (i) Matos, M. S.; Hofkens, J.; Verheijen, W.; De Schryver, F. C.; Hecht, S.; Pollak, K. W.; Fréchet, J. M. J.; Forier, B.; Dehaen, W. *Macromolecules* **2000**, *33*, 2967. (k) Weyermann, P.; Diederich, F. *Helv. Chim. Acta* **2002**, *85*, 599. (l) Van Doorslaer, S.; Zingg, A.; Schweiger, A.; Diederich, F. *ChemPhysChem* **2002**, *3*, 65.
- (8) For examples, see: (a) Issberner, J.; Vögtle, F.; De Cola, L.; Balzani, V. *Chem.—Eur. J.* **1997**, *3*, 706. (b) Kawa, M.; Fréchet, J. M. J. *Chem. Mater.* **1998**, *10*, 286. (c) Gorman, C. B.; Hager, M. W.; Parkhurst, B. L.; Smith, J. C. *Macromolecules* **1998**, *31*, 815. (d) Cardona, C. M.; Kaifer, A. E. *J. Am. Chem. Soc.* **1998**, *120*, 4023. (e) Vögtle, F.; Plevois, M.; Nieger, M.; Azzellini, G. C.; Credi, A.; De Cola, L.; De Marchis, V.; Venturi, M.; Balzani, V. *J. Am. Chem. Soc.* **1999**, *121*, 6290. (f) Gorman, C. B.; Smith, J. C. *J. Am. Chem. Soc.* **2000**, *122*, 9342. (g) Koenig, S.; Muller, L.; Smith, D. K. *Chem.—Eur. J.* **2001**, *7*, 979. (h) Stone, D. L.; Smith, D. K.; McGrail, P. T. *J. Am. Chem. Soc.* **2002**, *124*, 856. (i) Goldsmith, J. I.; Takada, K.; Abruna, H. D. *J. Phys. Chem. B* **2002**, *106*, 8504.
- (9) (a) Vinogradov, S. A.; Wilson, D. F. *Adv. Exp. Med. Biol.* **1997**, *428*, 657. (b) Vinogradov, S. A.; Lo, L. W.; Wilson, D. F. *Chem.—Eur. J.* **1999**, *5*, 1338. (c) Vinogradov, S. A.; Wilson, D. F. *Chem.—Eur. J.* **2000**, *6*, 2456. (d) Rozhkov, V.; Wilson, D. F.; Vinogradov, S. *Macromolecules* **2002**, *35*, 1991.
- (10) For review, see: Lash, T. D. Syntheses of novel porphyrinoid chromophores. In *The Porphyrin Handbook*; Kadish, K. M., Smith, K. M., Guillard, R., Eds.; Academic Press: New York, 2000.
- (11) *Handbook of Fluorescent Probes and Research Products*, Web edition at: <http://www.probes.com/handbook/Ch.21>; Molecular Probes, Inc.

- (12) (a) Hägerhäll, C. *Biochim. Biophys. Acta* **1997**, *1320*, 107. (b) Galkin, A. S.; Grivnennikova, V. G.; Vinogradov, A. D. *FEBS Lett.* **1999**, *451*, 157.
- (13) Senge, M. O. Highly substituted porphyrins. In *The Porphyrin Handbook*; Kadish, K. M., Smith, K. M., Guillard, R., Eds.; Academic Press: New York, 2000.
- (14) Lash, T. D. *J. Porphyrins Phthalocyanines* **2001**, *5*, 267.
- (15) Hambricht, P. Chemistry of water soluble porphyrins. In *The Porphyrin Handbook*; Kadish, K. M., Smith, K. M., Guillard, R., Eds.; Academic Press: New York, 2000.

values, when extracted from the titration curves, are subject to significant errors. It is more convenient to use instead apparent constants ( $pK$  or  $pK_{1/2}$ ),<sup>16</sup> which represent a somewhat averaged proton affinity of the macrocycle. The averaged  $pK$ 's are more reproducible and entirely adequate for drawing the comparisons between different types of porphyrins.

$pK$ 's of many water-soluble porphyrins have been measured<sup>15</sup> and shown to be dependent on the electronic effects of substituents, macrocycle planarity,<sup>17</sup> and the peripheral charges surrounding the protonation site.<sup>9c,16,18</sup> Any one of these factors, or all of them together, can be used to tune  $pK$ 's of porphyrins and to bring them into the desired range.

Compared to regular tetraarylporphyrins ( $Ar_4P$ ), porphyrins with extended  $\pi$ -conjugation exhibit considerable red-shifts of absorption and emission bands in both free-base and dicationic forms. In the case of tetraaryltetrabenzoporphyrins ( $Ar_4TBP$ ), the simplest representatives of symmetrically  $\pi$ -extended  $Ar_4P$ s, such red shifts of the Soret bands are in the range of 40–50 nm.<sup>10,14</sup>



The positions of the bands can be further adjusted by adding electron-donating or electron-withdrawing substituents X and/or Y. Such a large spectral separation makes it feasible to measure the fluorescence of  $Ar_4TBPs$  in the presence of  $Ar_4Ps$  and vice versa, by means of differential excitation, completely avoiding the interference between the spectra. Provided that solubilizing substituents (e.g. dendrons) can be attached to both  $Ar_4Ps$  and  $Ar_4TBPs$  and that the  $pK$ 's of both chromophors can be brought into the desired pH interval, such a pair of porphyrin dendrimers can be extremely useful for biological pH measurements.

In this paper we present the studied spectroscopic properties and protonations of a fluorescent dye couple, consisting of a porphyrin dendrimer and a tetrabenzoporphyrin dendrimer. The tetrabenzoporphyrin dendrimer reported in this work is the first example of a dendrimer with a free-base tetrabenzoporphyrin core<sup>19</sup>—a new water-soluble, fluorescent, near infrared dye.

## Results and Discussion

**Porphyrin Cores.** Porphyrins from two basic classes, i.e., *meso*-tetraarylporphyrins ( $Ar_4P$ ) and *meso*-tetraaryltetrabenzoporphyrins ( $Ar_4TBP$ ), were chosen for this study as cores for

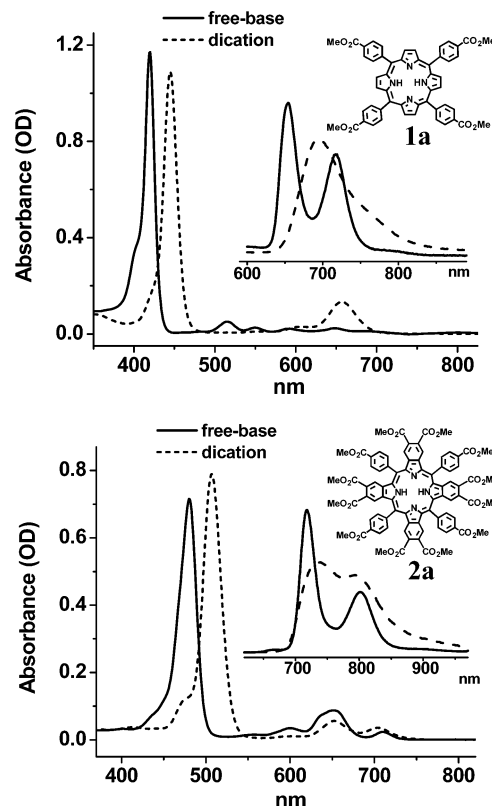


**Figure 1.** Structures and optical spectra of *meso*-tetrakis((methoxycarbonyl)phenyl)porphyrin (**1a**) and dodecakis(methoxycarbonyl)tetraphenyltetrabenzoporphyrin (**2a**) in  $CH_2Cl_2$  solutions. Insets show the corrected fluorescence spectra. Porphyrin dications were formed upon addition of TFA.

**Table 1.** UV–Vis and Fluorescence Spectroscopic Data for **1a** and **2a**<sup>a</sup>

compd	$\lambda_{Soret}$ (nm)	$\lambda_Q$ (nm)	$\lambda_{emis}$ (nm) ( $\lambda_{excit}$ )	$\phi_f$ (%)
<b>1a</b> fb <sup>b</sup>	419	514, 548, 590, 646	654, 717 (515)	15.3 ± 1.3
<b>1a</b> dc <sup>c</sup>	441	657	695 (462)	21.9 ± 1.6
<b>2a</b> fb <sup>b</sup>	480	509, 652, 703	718, 803 (490)	5.9 ± 0.8
<b>2a</b> dc <sup>c</sup>	510	652, 711	739, 801 (490)	8.3 ± 0.2

<sup>a</sup> Abbreviations: fb, free base; dc, dication. <sup>b</sup> Solution in  $CH_2Cl_2$ . <sup>c</sup> Solution in  $CH_2Cl_2/TFA$ .

dendrimers. The structures and the spectra of the selected representatives are shown in Figure 1, and the spectroscopic data are summarized in Table 1. The synthetic details are discussed in the following section.

The Soret bands of **1a** and **2a** free bases (fb) are 60 nm apart. Upon protonation both peaks shift by about 20–30 nm to the red, which ensures their minimal overlap in dicationic forms as well. The extinction coefficients at the Soret maxima of both porphyrins, i.e.,  $\log \epsilon_{Soret}^{1fb} = 5.6$  and  $\log \epsilon_{Soret}^{2fb} \sim 4.9$  (in  $CH_2Cl_2$ ), provide a means for efficient excitation. Upon protonation, four visible Q-bands of the free-base **1a** merge into a single peak at 657 nm. A similar transformation occurs with the somewhat less resolved bands of **2a**, which give rise to two distinct peaks at 652 and 711 nm. Maxima of **2a** dication (dc) differ much less from those of the free base than in the case of **1a**. This is perhaps a consequence of a much weaker structural deformation upon protonation in the case of the already severely distorted  $Ar_4TBP$  macrocycle.<sup>20</sup> In tetraarylporphyrins ( $Ar_4P$ )

(20) Finikova, O.; Cheprakov, A.; Carroll, P.; Dalosto S.; Vinogradov, S. *Inorg. Chem.* **2002**, *41*, 6944.

(16) Valiotti, A.; Adeyemo, A.; Williams, R. F. X.; Ricks, L.; North, J.; Hambright, P. *J. Inorg. Nucl. Chem.* **1981**, *43*, 2653.

(17) (a) Medforth, C. J.; Smith, K. M. *Tetrahedron Lett.* **1990**, *31*, 5583. (b) Barkigia, K. M.; Berber, M. D.; Fajer, J.; Medforth, C. J.; Renner, M. W.; Smith, K. M. *J. Am. Chem. Soc.* **1990**, *112*, 8851. (c) Takeda, J.; Ohya, T.; Sato, M. *Inorg. Chem.* **1992**, *31*, 2877.

(18) Kohata, K.; Higashio, H.; Yamaguchi, Y.; Koketsu, M.; Odashima, T. *Bull. Chem. Soc. Jpn.* **1994**, *67*, 668.

(19) A series of Pd tetrabenzoporphyrin dendrimers for in vivo oxygen imaging were recently synthesized: Rietveld, I.; Kim, E.; Vinogradov, S. *Tetrahedron* **2003**, in press.

such deformations are rather large, since  $Ar_4P$  dications typically have pronounced saddle-type geometries,<sup>21</sup> while the  $Ar_4P$  free bases are nearly flat.

Fluorescence spectra of both **1a** and **2a** (Figure 1, insets) also undergo hypochromic shifts upon protonation, although overlaps between the emission bands of the free-base and dicationic forms are more severe, especially in the case of **2a**. Importantly, the fluorescence quantum yield of **1a** (15.3%) is more than two times higher than that of **2a** (5.9%), which implies that larger quantities of the latter dye and/or stronger excitation should be used to obtain equal fluorescence responses. In dicationic form, the differences between the quantum yields of the dyes remain about the same. The diminished fluorescence of **2a** is probably due to its strong nonplanar distortion, which is typical for  $Ar_4$ -TBPs.<sup>20,22</sup> The distortion is known to increase the nonradiative pathways of excited-state deactivation.<sup>23</sup> On the other hand, the fluorescence of **2a** appears to be considerably stronger than that of similarly distorted but not  $\pi$ -fused porphyrins, such as tetracyclohexanoporphyrins.<sup>23a</sup> The reason for this increase is probably the enhanced rigidity of the tetrabenzoporphyrin macrocycle due to  $\pi$ -conjugation, which leads to a lower probability of thermal deactivation. One should keep in mind, however, that the quantum yield values obtained for tetrabenzoporphyrins are generally less accurate because of the rapidly fading efficiency of detection systems above 750–800 nm. This is true even in the case of the specially IR-enhanced PMT (Hamamatsu R2658P) used in our experiments.

The hydrolysis of the ester groups in both porphyrins produces water-soluble *meso*-tetracarboxyphenylporphyrin (**1b**) and dodecacarboxytetraphenyltetrabenzoporphyrin (**2b**). Despite the presence of several carboxylic groups, **1b** and even **2b** are still quite hydrophobic and readily aggregate in aqueous solutions upon acidification (pH < 5). The  $pK_3$  of **1b** has been reported to have a value of 5.5,<sup>15</sup> while the second constant  $pK_4$  could not be measured due to the aggregation. The relatively high value of  $pK_3$  of **1b** is likely to be caused by the four negatively charged peripheral carboxylates. Similar uncharged tetraarylporphyrins usually exhibit much lower  $pK$ 's (2–4).<sup>15</sup> The apparent  $pK$  of **2b**, determined by spectrophotometric titration, has a value of 7.3,<sup>20</sup> which represents a combination of two poorly resolved sequential protonations with  $pK_3 = 7.9$  and  $pK_4 = 6.4$ . In this case, high  $pK$  values are due to the combined effect of electrostatic shielding by ionized carboxylates, as in the case of **1b**, and the enhanced coupling of the carboxylates with the protonation site via the  $\pi$ -conjugated benzo rings. Blocking all 12 carboxylates with methoxypoly(ethylene glycol) residues results in a drop of  $pK$  by about 5 pH units.<sup>20</sup> Such a strong change indicates that tetrabenzoporphyrins with several electron-withdrawing groups are intrinsically very acidic—much more so than other nonplanar porphyrins.<sup>13,17</sup> On the other hand, although the apparent  $pK$  of **2b** itself falls into the desired interval (pH = 6–8), this porphyrin could not be used in

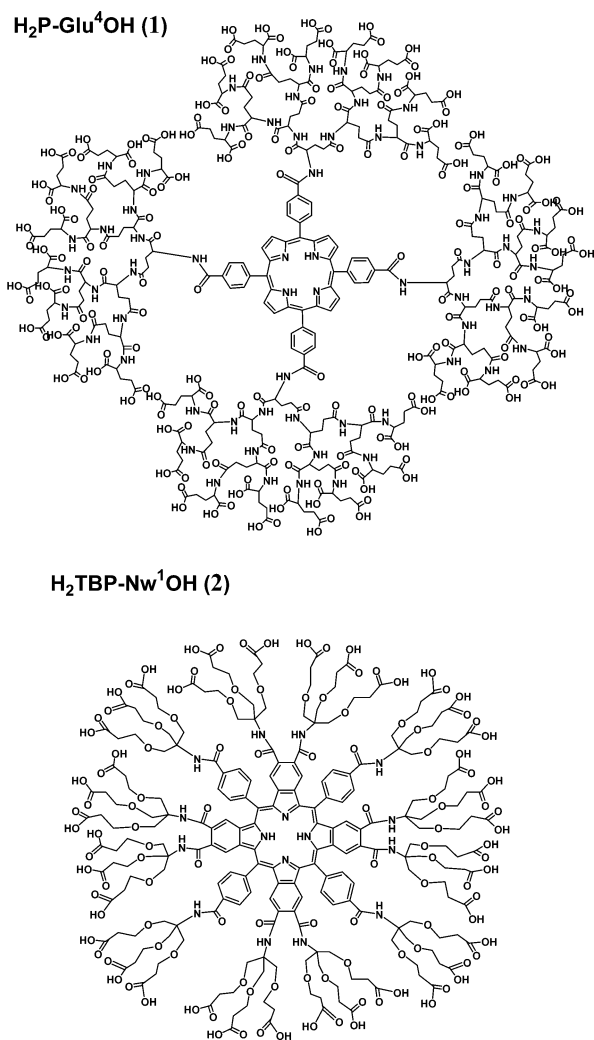


**Figure 2.** Structures of H<sub>2</sub>P-Glu<sup>4</sup>OH (MW 8532) (**1**) and H<sub>2</sub>TBP-Nw<sup>1</sup>OH (MW 5172) (**2**).

practical measurements due to its strong lipophilic nature. Not only does **2b** aggregate upon acidification, but it also binds to phospholipid membranes, which affects its fluorescent properties. Our attempts to prepare liposomes in the presence of **2b** resulted in the extraction of the porphyrin into the lipid phase, where its fluorescence was almost insensitive to the pH changes in the medium. It was, therefore, necessary to create a hydrophilic surrounding shell around the tetrabenzoporphyrin **2b** to prevent its aggregation and improve its solubility.

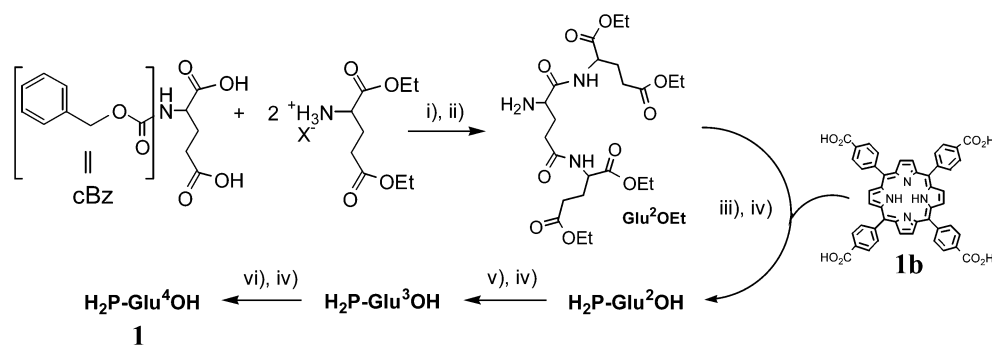
**Synthesis of Porphyrin Dendrimers.** As mentioned in the Introduction, a convenient method for the solubilization and isolation of porphyrins in the aqueous phase is dendritic encapsulation. For our particular case, employing dendritic encapsulation had one extra advantage, namely, the possibility to use peripheral charges on dendrimers to tune the  $pK$ 's of the central cores. With that in mind, porphyrin **1b** and tetrabenzoporphyrin **2b** were modified with dendritic ligands. The structures of two newly synthesized porphyrin dendrimers are shown in Figure 2.

Compound **1** is the generation 4 (Gen 4) polygutamic dendrimer with **1b** as a core, and **2** is the Gen 1 Newkome-type poly(ester amide) dendrimer with **2b** as a core. Compound **2** is, to our knowledge, the first free-base  $Ar_4$ TBP-core dendrimer.<sup>19</sup> It can be viewed as an intermediate structure

(21) (a) Stone, A.; Fleisher, E. B. *J. Am. Chem. Soc.* **1968**, *90*, 2735. (b) Cheng, B.; Munro, O. Q.; Marques, H. M.; Scheidt, W. R. *J. Am. Chem. Soc.* **1997**, *119*, 10732.

(22) Cheng, R. J.; Chen, Y. R.; Wang, S. L.; Cheng, C. Y. *Polyhedron* **1993**, *12*, 1353.

(23) (a) Gentemann, S.; Medforth, C. J.; Forsyth, T. P.; Nurco, D. J.; Smith, K. M.; Fajer, J.; Holten, D. *J. Am. Chem. Soc.* **1994**, *116*, 7363. (b) Gentemann, S.; Medforth, C. J.; Ema, T.; Nelson, N. Y.; Smith, K. M.; Fajer, J.; Holten, D. *Chem. Phys. Lett.* **1995**, *245*, 441. (c) Sazanovich, I. V.; Galievsky, V. A.; van Hoek, A.; Schaafsma, T. J.; Malinovsky, V. L.; Holten, D.; Chirvony, V. S. *J. Phys. Chem. B* **2001**, *105*, 7818.

Scheme 1<sup>a</sup>

<sup>a</sup> Key: (i) DCC, pyridine, THF, rt, 48 h; (ii) H<sub>2</sub>, Pd/C, THF/MeOH, rt, 72 h, 65%; (iii) DCC, pyridine, DMF, rt, 72 h, 75%; (iv) LiOH/THF/MeOH, rt, 95%; (v) DCC, pyridine, DMF, rt, 7 days, 53%; (vi) DCC, pyridine, 18-crown-6, DMF, 45 °C, 21 days, 37%.

between porphyrin dendrimers and phthalocyanine dendrimers,<sup>24</sup> and constitutes yet another example of a photoactive core dendrimer with near-infrared absorption and luminescence. Compounds **1** and **2** and the related porphyrin dendrimers are also abbreviated in the text as H<sub>2</sub>P-Glu<sup>4</sup>OH and H<sub>2</sub>TBP-Nw<sup>1</sup>-OH, where H<sub>2</sub>P and H<sub>2</sub>TBP refer to the core porphyrin **1b** and core tetrabenzoporphyrin **2b**, Glu<sup>4</sup> and Nw<sup>1</sup> designate polyglutamic and Newkome type poly(ester amide) dendrimers of generations 4 and 1, respectively, and OH represents the terminal groups.

The attachment of dendritic wedges to the porphyrins required initial modification of the macrocycles with suitable functional groups. Porphyrin **1b** could be easily prepared via Alder–Longo condensation<sup>25</sup> of pyrrole and 4-(methoxycarbonyl)benzaldehyde and subsequent hydrolysis. The symmetrically positioned carboxyl groups on *meso*-phenyl rings allowed for the coupling of four amino-terminal dendrons using conventional DCC chemistry. Polyglutamic and poly(ester amide) dendritic derivatives of **1b** have been synthesized in the past using this method.<sup>9a,d,e</sup> In our own previous work we used the divergent method to produce polyglutamic dendrimers with **1b** as a core, which succeeded up to Gen 3.<sup>9c</sup> Since an increase in the number of charges on the dendrimer periphery has been shown to shift the protonation p*K*'s of porphyrins in the desired direction, we attempted, in this work, the synthesis of even larger polyglutamic dendrimers, i.e., H<sub>2</sub>P-Glu<sup>4</sup>OEt and H<sub>2</sub>P-Glu<sup>4</sup>OH (**1**). Our initial intention was to switch entirely to the convergent route, which is known to give dendrimers with the highest monodispersity.<sup>1a,c</sup> The convergent scheme could be implemented via the method of synthesis of polyglutamic dendrons reported earlier.<sup>26,9d</sup> Using this approach we were able to produce appropriate amounts of the Gen 2 dendron; however, the isolation of the Gen 3 heptaglutamic dendron proved in our hands to be impractical due to low yields and a tedious purification process. Therefore, **1** was prepared by employing a combination of the convergent and divergent methods, following Scheme 1.

At first, the Gen 2 triglutamic dendron Glu<sup>2</sup>OEt was synthesized convergently in 65% yield. Condensation of Glu<sup>2</sup>-

OEt with **1b** gave the Gen 2 compound H<sub>2</sub>P-Glu<sup>2</sup>OEt in 75% yield, and the subsequent hydrolysis nearly quantitatively afforded polycarboxylic acid H<sub>2</sub>P-Glu<sup>2</sup>OH. Further synthesis of the Gen 3 compound H<sub>2</sub>P-Glu<sup>3</sup>OH followed the divergent path described earlier.<sup>9c</sup> Attachment of the next layer of glutamates to 32 terminal carboxyl groups on H<sub>2</sub>P-Glu<sup>3</sup>OH, however, presented a significant obstacle due to the complete insolubility of this compound in organic solvents. This problem was due in part to the fact that Gen 3 porphyrin dendrimer could be isolated only as a poly-Na<sup>+</sup> or -K<sup>+</sup> salt (H<sub>2</sub>P-Glu<sup>3</sup>O<sup>-</sup>M<sup>+</sup>) and not as a free carboxylic acid. Hoping to facilitate the uptake of H<sub>2</sub>P-Glu<sup>3</sup>O<sup>-</sup>K<sup>+</sup> into the liquid organic phase, we attempted to use 18-crown-6 polyether, which proved to be an effective strategy. Although the coupling of diethyl glutamates to H<sub>2</sub>P-Glu<sup>3</sup>OH still required a lengthy reaction time (21 days), the progress of the synthesis could already be detected soon after the addition of the crown ester to the reaction mixture, as the purple porphyrin became gradually extracted into the liquid phase. As a result, the Gen 4 ethyl ester terminated dendrimer H<sub>2</sub>P-Glu<sup>4</sup>-OEt could be synthesized in 37% yield. The MALDI-TOF spectrum of this compound (MW 10326) revealed a distribution of peaks spaced between 10349 (M<sup>+</sup> + Na) and ~8500 and separated by 314 MW units. Notably, this mass difference is most likely due to the fragmentation of the dendrimer rather than to the presence of underderivatized products. The latter would appear if some of the carboxyl groups on H<sub>2</sub>P-Glu<sup>3</sup>OH did not undergo coupling with diethyl glutamates. Such “defective” dendrimers would give rise to the mass peaks decremented in steps of 185 but not 314 units. Similar patterns have been observed in the spectra of Pd tetrabenzoporphyrin dendrimers, produced in the complementary syntheses.<sup>19</sup> H<sub>2</sub>P-Glu<sup>4</sup>OEt was smoothly hydrolyzed under basic conditions, and the resulting poly-Na<sup>+</sup> salt of H<sub>2</sub>P-Glu<sup>4</sup>OH (**1**) was isolated as a fluffy green hygroscopic powder. Compound **1** has in total 60 glutamic units and 64 peripheral carboxylate groups.

While Ar<sub>4</sub>P<sub>s</sub> with various substituents are readily available, synthesis of functionalized Ar<sub>4</sub>TBP<sub>s</sub> has long presented a significant challenge.<sup>10</sup> Recently, two improved methods were proposed, charting the routes to Ar<sub>4</sub>TBP<sub>s</sub> with various peripheral functional groups.<sup>27,28</sup> In this work we made use of one of these methods,<sup>28</sup> which is advantageous because of its inexpensive starting materials and shorter reaction sequence. The synthesis

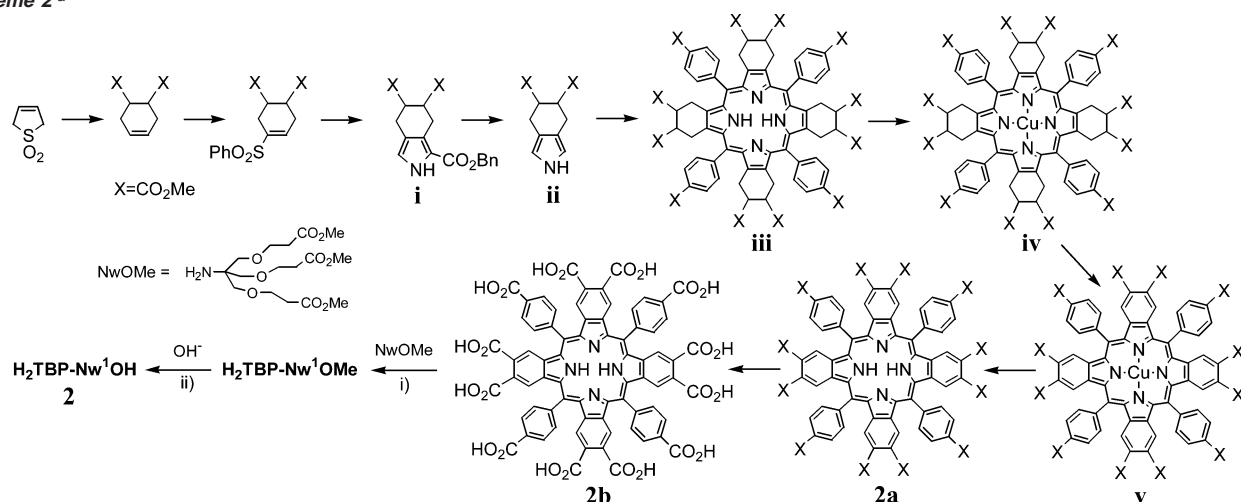
(24) (a) Kimura, M.; Nakada, K.; Yamaguchi, Y.; Hanabusa, K.; Shirai, H.; Kobayashi, N. *Chem. Commun.* **1997**, 1215. (b) Brewis, M.; Clarkson, G. J.; Goddard, V.; Helliwell, M.; Holder, A. M.; McKeown, N. B. *Angew. Chem., Int. Ed.* **1998**, *37*, 1092. (c) Kimura, M.; Sugihara, Y.; Muto, T.; Hanabusa, K.; Shirai, H.; Kobayashi, N. *Chem.—Eur. J.* **1999**, *5*, 3495. (d) Brewis, M.; Helliwell, M.; McKeown, N. B.; Reynolds, S.; Shawcross, A. *Tetrahedron Lett.* **2001**, *42*, 813.

(25) Adler, A. D.; Longo, F. R.; Shergalis, W. D. *J. Am. Chem. Soc.* **1964**, *86*, 3145.

(26) Twyman, L.; Beezer, A. E.; Mitchell, J. C. *Tetrahedron Lett.* **1994**, *35*, 4423.

(27) (a) Ito, S.; Murashima, T.; Uno, H.; Ono, N. *Chem. Commun.* **1998**, 1661. (b) Ito, S.; Uno, H.; Murashima, T.; Ono, N. *Tetrahedron Lett.* **2001**, *42*, 45.

(28) Finikova, O.; Cheprakov, A.; Beletskaya, I.; Vinogradov, S. *Chem. Commun.* **2001**, 261.

Scheme 2<sup>a</sup>

<sup>a</sup> Key: (i) DCC, BtOH, *sym*-collidine, DMF, 0 °C, 4 days, 81%; (ii) NaOH/MeOH, 30 min, 95%. See ref 28 and the Experimental Section for the details of the syntheses leading to the core tetrabenzoporphyrin **2b**.

of the core **2b**, shown in Scheme 2, generally followed the protocol reported earlier. The critical step in this method is the oxidative aromatization of the preceding tetraarylporphyrin ( $Ar_4TCHP$ , iv) into the  $Ar_4TBP$  (v) by DDQ. The reaction is very sensitive to the solvent, and in the case of the porphyrin shown, it must be carried out in acetonitrile. Important is also the choice of Cu as a temporary metal in  $Ar_4TCHP$  (iv) for promoting the oxidation. Aromatization is impossible when  $Ar_4TCHPs$  are taken as free bases. Acidification of the medium, which instantly follows the addition of DDQ, leads to the virtually immediate formation of  $Ar_4TCHP$  dications, reflecting the extremely high basicity of these porphyrins.<sup>20</sup> The dications are totally inactive in aromatization, and the entire process stops. Therefore, it is important to block  $Ar_4TCHPs$  with such metal ions that, on one hand, the formed metalloporphyrins are stable enough to sustain aromatization but, on the other hand, the metal can be pulled back out to give the  $Ar_4TBP$  free bases.

Synthesis of **2b** was succeeded by the attachment of 12 Newkome fragments NwOMe.<sup>29</sup> This was accomplished using standard peptide chemistry. The Newkome building block resembles glutamate in its composition but offers the advantage of a higher branching number (BN = 3) and therefore faster dendrimer expansion with increasing generations. The dodeca-substituted core combined with Newkome fragments allowed us to build the dendrimer  $H_2TBP-Nw^1OMe$  (**2c**) with 36 peripheral methoxycarbonyl groups (MW 5676) in a single coupling step. The purification of **2c** was accomplished by GPC on Biorad S-X1 beads, generating material of quite high purity. The MALDI-TOF spectrum of the sample revealed that the compound was contaminated with only about 5% of the satellite carrying one less Newkome dendron.

Hydrolysis of **2c** gave the water-soluble compound  $H_2TBP-Nw^1OH$  (**2**) in a nearly quantitative yield. Similar to compound **1**, **2** could not be precipitated from the aqueous solution even upon strong acidification, and therefore, the solution had to be purified from the excess salt by extensive dialysis. Subsequent lyophilization produced the green hygroscopic powder **2**.

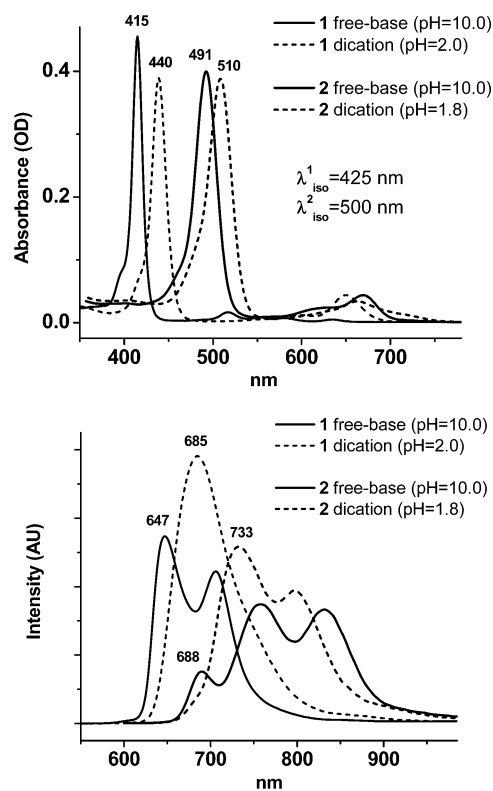


**Figure 3.** Absorption and corrected fluorescence spectra of porphyrin dendrimers  $H_2P-Glu^uOH$  (**1**) and  $H_2TBP-Nw^1OH$  (**2**) in aqueous solutions.

### Properties of Porphyrin Dendrimers and pH Titrations.

Both compounds **1** and **2** are extremely water soluble and do not precipitate through the entire pH range. We also could not observe any spectroscopic evidence for aggregation of the porphyrin dendrimers between pH 2 and pH 10.

The absorption and emission spectra of the compounds, as well as the titration curves resulting from fluorescence rationing, are shown in Figures 3 and 4. The excitation of fluorescence in both cases was carried out at the isosbestic points in the Soret regions, i.e., at 425 and 500 nm, respectively. The spectroscopic data and the  $pK$ 's obtained from the changes in absorption and emission spectra, as well as the comparative data for some reference compounds, are summarized in Table 2.

(29) (a) Newkome, G. R.; Lin, X. *Macromolecules* **1991**, *24*, 1443. (b) Newkome, G. R.; Lin, X.; Young, J. K. *Synlett* **1992**, 53.

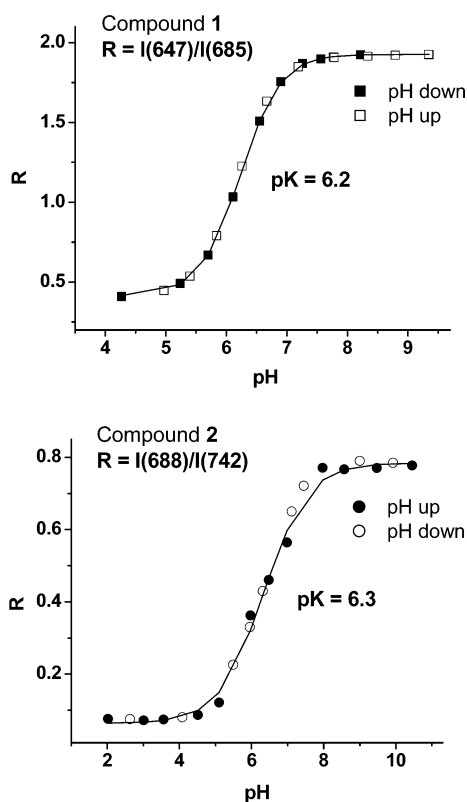


**Figure 4.** Titration curves for porphyrin dendrimers **1** and **2** obtained from rationing fluorescence intensities at the selected wavelengths. “pH down” and “pH up” indicate the direction in pH change during the titration, i.e., from basic to acidic and vice versa.

**Table 2.** Photophysical Data and Apparent Protonation Constants for Porphyrin Dendrimers **1** and **2** and Related Reference Compounds

compd	$\lambda^{\text{fb}}_{\text{Soret}}$ (nm), $\lambda^{\text{dc}}_{\text{Soret}}$ (nm) <sup>a</sup>	$\text{p}K_{\text{abs}}^b$ ( <i>n</i> )	$\text{p}K_{\text{fluo}}(\lambda^1_{\text{max}}, \lambda^2_{\text{max}})^c$	$\phi_{\text{fl}}$ (%)
H <sub>2</sub> P-Glu <sup>4</sup> OH ( <b>1</b> )	416, 440	6.4 (0.9)	6.2 (647, 685)	18.4 (fb); 36.2 (dc)
H <sub>2</sub> P-Glu <sup>2</sup> OH	415, 437	5.4 (1.0)		
H <sub>2</sub> P-Glu <sup>2</sup> PEG350 <sup>d</sup>	416, 438	2.5 (1.1)		
H <sub>2</sub> TBP-Nw <sup>1</sup> OH ( <b>2</b> )	491, 510	5.6 (0.6)	6.3 (688, 742)	5.2 (fb); 13.6 (dc)
<b>2b</b> <sup>e</sup>	478, 496	7.3 (0.6)	7.2 (808, 728)	
<b>2b</b> -(PEG350) <sub>12</sub> <sup>e</sup>	475, 494	2.2 (1.1)		

<sup>a</sup> Abbreviations: fb, free base; dc, dication. <sup>b</sup> Apparent  $\text{p}K_{\text{abs}}$  obtained via rationing absorbance at the Soret peak of a free base ( $\lambda^{\text{fb}}_{\text{Soret}}$ ) to the absorbance at the isosbestic point throughout the entire protonation range and fitting the points with Hasselbach equation with nonfixed parameter *n*. <sup>c</sup>  $\text{p}K_{\text{fluo}}$  obtained via rationing intensities of emission at the wavelength  $\lambda^1_{\text{max}}$  and  $\lambda^2_{\text{max}}$ , as shown in Figure 4, and analyzing the data in the same way as for absorption. <sup>d</sup> H<sub>2</sub>P-Glu<sup>2</sup>PEG350 is a polyglutamic porphyrin dendrimer with PEG350 terminal residues, where PEG350 designates methoxypoly(ethylene monomethyl ether) with average MW 350. See the Experimental Section for details. <sup>e</sup> Data are taken from the ref 20. **2b**-(PEG350)<sub>12</sub> is **2b** esterified with 12 PEG350 residues—a water-soluble uncharged analogue of the core porphyrin **2b**.

The spectra of the porphyrin dendrimers resemble those of the cores, although, typical of water-soluble porphyrins, the bands in aqueous solutions are broadened. In the case of compound **2** and the other two tetrabenzoporphyrins (see footnote *d*, Table 2), the significant differences among the absorption maxima are most likely caused by electronic factors, since the carboxyl groups at the periphery are coupled directly to the macrocycles through the conjugated  $\pi$ -system. In contrast, the three H<sub>2</sub>P dendrimers shown are different from one another only by the groups which are quite distant from the porphyrin cores, and therefore, the cores are spectroscopically insensitive to these differences. The dendritic cages themselves, on the other hand,

seem to produce no spectroscopic effect on the encapsulated cores. It appears that in compound **1** and in the reference Gen 2 dendrimers the attached branches seem to have almost no influence on the porphyrin absorption bands. (For comparison, the maxima of the core H<sub>2</sub>TCP (1b) in water are  $\lambda^{\text{fb}}_{\text{Soret}}$  416 nm and  $\lambda^{\text{dc}}_{\text{Soret}}$  439 nm.) This indicates that polyglutamic dendrons maintain rather open conformations in aqueous solutions, leaving the porphyrins accessible to the solvent. On the other hand, the electrochemical<sup>7b,e</sup> and small-molecule diffusion<sup>9</sup> studies of porphyrin dendrimers, conducted earlier, reveal that polyglutamic and poly(ester–amide) cages do impose encapsulation constraints on the porphyrin cores. These constraints, while not very significant, are still perfectly measurable, indicating that electrochemical and kinetic methods are much more sensitive to the dendritic effects than static optical spectroscopy.

As mentioned above, the spectroscopic transitions observed during pH titrations of porphyrins can include two protonations, which may not be well resolvable if the corresponding  $\text{p}K$ 's fall close on the pH scale. A sigmoidal curve, obtained by plotting the ratio of absorbances vs pH, is, in this case, a superposition of individual protonations, weighted by different scaling factors. These factors depend on the actual magnitudes of the changes induced by each protonation in the spectra at the wavelengths selected. The product of the superposition usually resembles a sigmoidal curve too but with a wider span over the pH axis. If such a situation occurs, fitting the experimental data using the Hasselbach equation with the fixed parameter *n* = 1 (eq 1) would be incorrect. Instead, one should revert to an equation describing two sequential protonations or, alternatively, to use the standard Hasselbach equation (eq 1) but leaving the parameter *n* nonfixed. During the fitting process, *n* would automatically adapt a value lower than 1, resulting in an average apparent value for  $\text{p}K$ . The latter approach seems more reasonable when  $\text{p}K$ 's are close, as resolving two sequential protonations would require almost noiseless data.

In the eq 1, *B* and *C* are constants, related to the concentration of solution and to the extinction coefficients (or emission intensities) of the porphyrin at the wavelength(s) selected; *R*(pH) is the intensity of absorption (or emission) for either the free base or the dication as a function of pH. Alternatively, *R* can refer to the ratio of intensities at two selected wavelengths.

$$R(\text{pH}) = C \frac{10^{n(\text{pH}-\text{p}K)}}{1 + 10^{n(\text{pH}-\text{p}K)}} + B \quad (1)$$

In Table 2 we present the apparent absorption-derived ( $\text{p}K_{\text{abs}}$ ) and fluorescence-derived ( $\text{p}K_{\text{fluo}}$ ) constants obtained using eq 1 with nonfixed *n* and show them together with the corresponding parameters *n*. Using this type of analysis is justified in our case because protonations of the peripheral carboxylates in dendrimers additionally “smooth out” the shape of the protonation curve, making it more difficult to distinguish between the individual porphyrin protonations. Accordingly, the  $\text{p}K$ 's represent the weighted averages of two sequential protonations.

For compound **2** and the parent tetrabenzoporphyrin **2b** the *n* values reach as low as 0.6, revealing that the corresponding transitions encompass more than a single proton addition and that both protonations contribute significantly to the spectral changes at the selected wavelengths. The fluorescence-derived  $\text{p}K$ 's ( $\text{p}K_{\text{fluo}}$ ) are sensitive to the same effects as  $\text{p}K_{\text{abs}}$ , and if

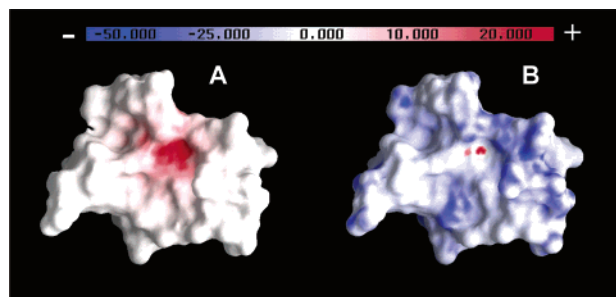


**Figure 5.** Maps of electrostatic potential (positive, red; negative, blue) of the Gen 3 porphyrin dendrimers dications:  $H_4P^{2+}$ -Glu $^3$ OH (A) with neutral surface;  $H_4P^{2+}$ -Glu $^3$ O $^-$  (B) with 32 peripheral ionized carboxylates.

the isosbestic points are not well defined, changing wavelengths for rationing usually results in slight  $pK$  shifts. This “imprefection” in the protonation curves also explains why the  $pK_{\text{fluo}}$  values in Table 2 differ somewhat from the  $pK_{\text{abs}}$  values. It also demonstrates that by carefully choosing the emission wavelengths for any particular measurement, one can emphasize one contributing protonation over another and thus shift the apparent  $pK_{\text{fluo}}$  value in the desired direction.

Both  $pK_{\text{abs}}$  and  $pK_{\text{fluo}}$  of compound **1** are much higher than would be normally expected for regular planar tetraarylporphyrins without donor substituents ( $pK = 2-4$ ). The electrostatic shielding by peripheral carboxylates, proposed earlier,<sup>9c</sup> is likely to be responsible for the  $pK$  shift in this case, as well as in the case of the Gen 2 dendrimer  $H_2P$ -Glu $^2$ OH ( $pK_{\text{abs}} = 5.4$ ).

The stabilization of the porphyrin dication by the surface charges on the surrounding dendrimer translates effectively into lowering of the core positive electrostatic potential and, therefore, decreasing the total free energy of the protonated porphyrin. An illustration of this effect could be obtained by calculating the maps of electrostatic potential on some arbitrary molecular surfaces and comparing the contour plots generated for the dications surrounded by protonated vs ionized peripheral carboxyls. Such plots, produced for Gen 3 porphyrin dendrimer dications  $H_4P^{2+}$ -Glu $^3$ OH (A) and  $H_4P^{2+}$ -Glu $^3$ O $^-$  (B), are shown in Figure 5.

To obtain these maps, we selected a relatively opened conformation of the dendrimer, in which one plane of the porphyrin is well seen. Sampling of the conformations was done by running molecular dynamics (MM+ force field, Hyperchem 5.0) at a relatively high temperature (1000 °C) in a vacuum, followed by geometry optimization of a few selected conformations. In the selected dications of porphyrin dendrimers the effective charges of +0.5 were assigned to all four inner-porphyrin protons, to more realistically approximate the charge distribution within the porphyrin cavity. In the case of fully ionized structure  $H_4P^{2+}$ -Glu $^3$ O $^-$  (B), the charges of -0.5 were assigned to all oxygen atoms in the terminal glutamic acid residues. Modeling of the surface potential was performed using Poisson-Boltzmann solver as implemented in GRASP software.<sup>30</sup> The solvent (water) was treated as a continuum with the dielectric constant of 80, and the concentration of salt was kept 0.1 M in both cases A and B.

The differences between the peripherally charged (A) and uncharged (B) forms of the dication  $H_4P^{2+}$ -Glu $^3$ OH are well seen in the figure. The plots in both cases were produced using

the same color scale, and the surfaces were drawn at the same distances from the atomic centers. The red color designates the areas of positive potential ( $+\delta\Psi$ ), induced by the protons attached to the imine nitrogens in the porphyrin cores. In the case of the dendrimer with no peripheral charges (A) the red spot and, therefore, the  $+\delta\Psi$  value are noticeably larger than in the peripherally ionized dendrimer (B). In the latter case, the negative (blue) charges partially compensate for the central positive charge, lowering the electrostatic energy of the dication and decreasing the total protonation free energy of the porphyrin.

To experimentally check whether the increase in  $pK$  was indeed due to the electrostatic stabilization of dications, we blocked the charges on the dendrimer  $H_2P$ -Glu $^2$ OH with neutral methoxypoly(ethylene glycol) fragments (PEG350), converting it into a still completely water-soluble but peripherally uncharged dendrimer  $H_2P$ -Glu $^2$ PEG350. As seen from the table, the result was a more than 3 pH units drop in  $pK$ , thus confirming our assumption. The power of the stabilization effect, however, seems to reduce rapidly with the distance separating these charges from the core. The difference between the  $pK$ 's of **1** ( $pK_{\text{abs}} = 6.4$ ) and  $H_2P$ -Glu $^2$ OH ( $pK_{\text{abs}} = 5.4$ ) is only 1 pH unit, while **1** has 48 carboxylates more than the Gen 2 dendrimer  $H_2P$ -Glu $^2$ OH. At the same time, just 16 charges on  $H_2P$ -Glu $^2$ -OH (compared to no charges on  $H_2P$ -Glu $^2$ PEG350) produce a much stronger effect, probably because of their closer proximity to the core.

In the case of **2** and the other two  $Ar_4$ TBPs, more factors than simple through-space electrostatic shielding affect the protonation  $pK$ 's. As mentioned above, tetrabenzoporphyrins are intrinsically less basic than regular porphyrins due to the extended  $\pi$ -conjugation.<sup>20</sup> A much higher than expected basicity of **2b** ( $pK_{\text{abs}} = 7.3$ ) is likely to be caused by a combination of the through-bond and through-space effects of adjacent carboxylates. As a result, the  $pK_{\text{abs}}$  of this porphyrin drops down to 2.2 when the peripheral groups are esterified with PEG350 chains (Table 2, compound **2b**-PEG350<sub>12</sub>). The 36 peripheral charges in **2**, provided by 12 Newkome dendrons, create another substantial stabilization shield around the central tetrabenzoporphyrin dication, bringing its  $pK_{\text{abs}}$  up to 5.6 and the  $pK_{\text{fluo}}$  to 6.3.

As seen in Figure 3, the overlap between the Soret bands of the porphyrin dendrimers **1** and **2** is rather small, making it possible to use the corresponding isosbestic points ( $\lambda_{\text{max}} = 425$  nm and  $\lambda_{\text{max}} = 500$  nm) for differential excitation of fluorescence of the porphyrins. To test whether such a spectral separation is sufficient for independent pH determinations using the dyes simultaneously, we carried out a titration of a solution with both compounds **1** and **2**. The corresponding changes in the spectra are depicted in Figure 6.

In this case the emission measurements were performed using an instrument with a regular detector (Hamamatsu R928 vs IR-sensitive Hamamatsu R2658P), and so the shapes of the spectral lines are somewhat different from those shown in Figure 3. The insets show the pH-titration curves obtained by fluorescence rationing.

According to Table 2, the emission quantum yield of the dendrimer **2** is 3–4 times lower than that of **1**. To bring the fluorescence responses from the dyes to similar levels, the amounts taken into the mixture were adjusted, which is reflected by the relative intensities of the Soret absorptions in Figure 6A.

(30) Nicholls, A.; Sharp, K. A.; Honig, H. *Proteins* **1991**, *11*, 281.

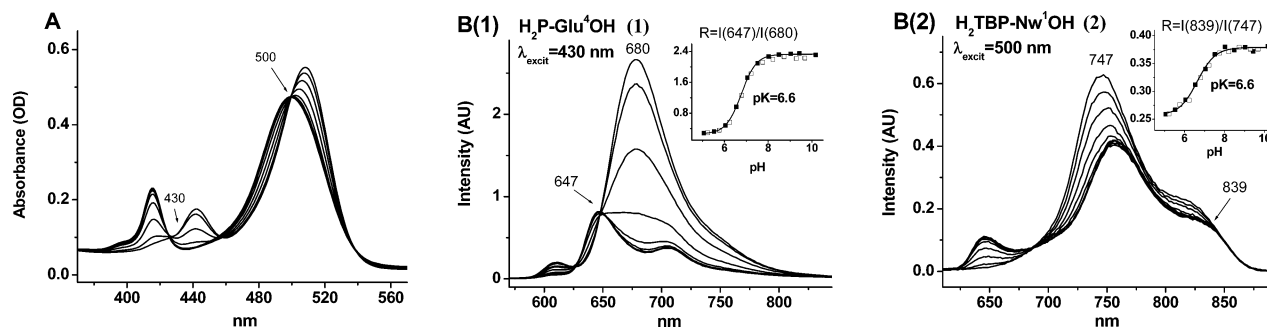


**Figure 6.** Absorption (A) and fluorescence (B(1) and B(2)) spectra upon titration of the mixture of  $\text{H}_2\text{P-Glu}^4\text{OH}$  (1) and  $\text{H}_2\text{TBP-Nw}^1\text{OH}$  (2). The wavelengths for fluorescence rationing were chosen to minimize the overlaps of responses from the compounds. The titrations were performed in a buffered (50 mM phosphate) solution.

The mixture contained about 4 times less of the porphyrin dendrimer **1**. The excitation of fluorescence of **1** was carried out at 430 nm, which is 5 nm off the absorption isosbestic point. This emphasized the dication emission relative to that of the free base and provided a cleaner isosbestic point at 647 nm in the fluorescence spectrum (Figure 6B(1)). As seen from Figure 6B(1), the fluorescence spectrum of **1** is practically undisturbed throughout the entire pH range, even in the presence of a large excess of **2**. The ratiometric curve (inset) is smooth and can be used for pH measurements between pH 6 and 8 ( $pK = 6.6$ ).

When excited at 500 nm, the fluorescence of the mixture consists mainly of the spectrum of dendrimer **2**. At basic pH, there is, however, a small peak around 647 nm originating from **1**. This band is due to an overlap of the excitation with the absorption Q-band of **1** ( $\lambda_{\text{max}} = 517$  nm). Nevertheless, choosing wavelengths for fluorescence rationing ( $\lambda_1 = 747$  nm and  $\lambda_2 = 839$  nm) away from this peak allows one to monitor the titration curve of **2** exclusively. As in the case of **1**, rationing at different wavelengths (Figure 6B(2), inset) leads to a more basic  $pK = 6.6$  than in the individual titration of **2** ( $pK = 6.3$ ). Such a shift is caused by an admix of transitions due to the first and the second protonations in the fluorescence spectra and the resulting indistinct isosbestic points.

The titration experiment described above revealed that optically porphyrin dendrimers **1** and **2** do not interact and their protonations are spectroscopically independent. It therefore became of interest to model a system in which these dyes would be separated spatially but resolved only optically, permitting the monitoring of pH changes in separate microscopic compartments. As mentioned in the Introduction, proton compartmentalization is the key to metabolic energy conservation.<sup>31</sup> Precise quantification of proton transport processes is critical for understanding the function of biological machinery involved in bioenergetics. A phospholipid liposome with a reconstituted enzyme, i.e., a *proteoliposome*,<sup>32</sup> can serve as a mimic of a bacterial or mitochondrial membrane, in which the enzyme exists in its natural environment. If a function of the enzyme is to translocate protons across the membrane, the proton gradient is built upon the enzyme working cycle. The quantification of this gradient could be achieved if proton-sensitive optical probes are placed inside and outside the liposome, where they would report independently on pH changes. A system of this kind would require the reporters themselves to be membrane-

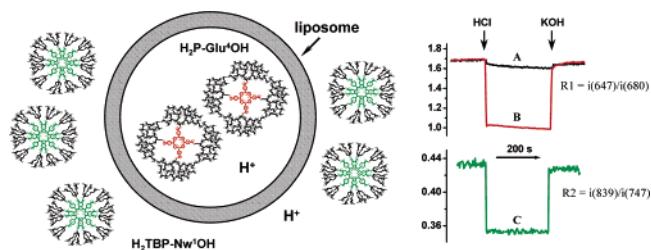


**Figure 7.** Phospholipid liposome with  $\text{H}_2\text{P-Glu}^4\text{OH}$  (1) captured inside and  $\text{H}_2\text{TBP-Nw}^1\text{OH}$  (2) contained in the outside solution (10 mM phosphate). Fluorescence changes vs time were recorded upon addition of acid (HCl) or base (KOH) (indicated by arrows). The amounts of acid and/or base were calibrated to produce 1 pH unit jumps: A (black), dye **1** (inside); B (red), dye **1** (inside) in the presence of 0.5 mg/mL of gramicidin; C (green), dye **2** (outside) in the presence or absence of gramicidin.

impermeable, and porphyrin dendrimers, like **1** and **2**, seem to be well suited to perform such a task.

Figure 7 shows a model system that we used to examine the applicability of porphyrin dendrimers for pH-gradient measurements.

Phospholipid liposomes were prepared by sonication of a phospholipid film, a standard technique used routinely in biochemical preparations.<sup>33</sup> The average diameter of liposomes prepared by this method is 20–30 nm, and the approximate diameter of **1** is about 20–30 Å.<sup>34</sup> This implies that only a few molecules of **1** can, in principle, fit inside each vesicle. It must be kept in mind, however, that at pH 7, and when the liposome concentration level is such that the combined liposome internal volume is, for example, 0.001 of the volume of the entire solution, only 1 out of 10 000 liposomes contains a proton. The concentration of the dye is usually at a submicromolar level ( $10^{-6}$ – $10^{-7}$  M), and so the distribution of the dye molecules is close to that of the protons, i.e., about  $10^{-3}$ – $10^{-4}$  dye molecules/liposome. Even though measuring a “single” proton with just a “single” molecule of a probe might at first glance appear unrealistic, averaging over a large number of vesicles produces the same effect as a regular ensemble averaging. Indeed, there are about  $10^{14}$  liposomes of 30 nm diameter/1 mL of solution at the assumed level of liposome concentration (0.001 of total volume), and the overall pH measurement, therefore, becomes macroscopic in nature.

The liposomes were prepared in a solution containing porphyrin dendrimer **1**, so the dye was included in the interior of

(31) Mitchell, P.; Moyle J. *Nature* **1967**, *213*, 137.

(32) Rigaud, J. L.; Pitard, B.; Levy, D. *Biochim. Biophys. Acta* **1995**, *1231*, 223.

(33) Driessen, A. J.M.; De Vrij, W.; Konings, W. N. *Eur. J. Biochem.* **1986**, *154*, 617.

(34) Molecular diameter was determined by taking a few measurements across the calculated dendrimer molecule and averaging the obtained distances.

the liposomes during the sonication process. To remove the outside dye, the liposomes were rigorously purified by chromatography on a Sephadex G200 column, which contained a layer of an anion-exchange resin at the bottom. The affinity of the anion-exchange resin to the carboxylate-terminated dendrimers is extremely high, allowing for complete removal of the dye traces from the outside solution. The controls were set by gentle centrifugation of the liposomes, followed by the fluorescence measurements of the supernatant solutions, which were found virtually fluorescence-free.

The liposomes containing dye **1** were placed in a 10 mM phosphate buffer where the second dye **2** was dissolved at pH 7.1. Acid and base additions (indicated by arrows in Figure 7) were precalibrated to produce 1.0 pH unit jumps, but the actual pH, measured by a conventional electrode, was also recorded continuously during the experiment. The fluorometer used in our measurements (SPEX Fluorolog-2) was equipped with just one PMT, permitting detection at only one wavelength at a time. Because fluorescence rationing requires measurements of intensities at two wavelengths, the emission monochromator had to be moved physically, which significantly increased the detection time. Since it was desirable to monitor the pH changes with at least 2 s time resolution, measurements with two dyes were accomplished in two independent experiments. These measurements, if performed in a single run, would require a much longer acquisition times, since the excitation monochromator in this case would have to be moved between the Soret bands of **1** and **2** and two more emission intensities would have to be measured. The changes in fluorescence ratios are shown in Figure 7.

The differences in responses of the outside and inside dyes (**1** and **2**, respectively) to the pH jumps in the medium are obvious. While dye **2** in the bulk instantaneously responded upon additions of acid or base, the signal originated from **1** kept changing only slightly, indicating that this dye was well isolated from the outside solution. A gradual decline of the ratio  $R_1$  (liposome-encapsulated porphyrin dendrimer **1**) upon addition of HCl reflects acidification of the liposome's internal space. This process is due to a slow diffusion of protons across the phospholipid membrane (Figure 7A). When proton channels were made in the membranes by a special pore-forming peptide gramicidin,<sup>35</sup> fluorescence of dye **1** inside the liposomes reacted immediately to the additions of acid or base (Figure 7B). Similar results were obtained when a combination of nigericin and valinomycin was used to make pores in the liposomes (not shown). Such pores permit free movement of the protons in and out of the liposomes, resulting in a fast equilibration of external and internal pH's. The pores, however, are too small for the porphyrin dendrimer molecules, so these remain captured inside the vesicles.<sup>36</sup> As expected, the fluorescence response of the outside dye **2** (ratio  $R_2$ ) appeared sensitive to the additions of HCl or KOH regardless of whether the pores were made in the liposomes (Figure 7C). This experiment clearly demonstrates that the pair of dyes **1** and **2** can be used to quantify proton concentrations inside and outside the vesicles using optical measurements in bulk solutions.

## Conclusions

In this paper we show that dendritic cages are effective in modulating porphyrin protonation constants ( $pK$ ). This effect is due to the peripheral charges on dendrimers, which are responsible for the stabilization of porphyrin dications. The resulting  $pK$ 's of normally quite acidic porphyrins can be moved into the physiological pH range (pH 6–8), suggesting the usefulness of porphyrin dendrimers as optical pH indicators. By synthesizing a polyglutamic porphyrin dendrimer with a tetraarylporphyrin ( $Ar_4P$ ) core and the dendritic tetraaryltetrabenzoporphyrin ( $Ar_4TBP$ ), we succeeded in demonstrating that in water solutions two porphyrinoid chromophores with dendritic jackets and nonoverlapping absorption and emission spectra do not interact optically and do not influence each other's protonation curves. The latter can be determined individually from the mixtures of the dyes using differential excitation/emission techniques. The peripheral charges on the dendrimers ensure complete membrane impermeability of the synthesized indicators, which was demonstrated by placing porphyrin dendrimers with two spectroscopically different cores inside and outside phospholipid vesicles and determining the pH in both compartments independently using bulk spectroscopic measurements. The synthesized dyes form an effective indicator pair for proton gradient determination. This is a new potential application for porphyrin dendrimers, which capitalizes on dendritic encapsulation as a tool for the isolation and solubilization of optically active cores, as well as on the modulation and tuning of their physicochemical properties.

## Experimental Section

**General Methods.**  $^1H$  and  $^{13}C$  spectra were recorded on a Varian Unity-500 spectrometer. Optical spectra were recorded on a Perkin-Elmer Lambda 35 UV/vis spectrophotometer, and fluorescence measurements were performed on a SPF-500C (SLM Instruments, Inc.) fluorometer, equipped with a Hamamatsu R928 PMT and on a SPEX Fluorolog-2 spectrofluorometer (Jobin-Yvon Horiba, Inc.), equipped with an infrared enhanced R2658P PMT. Matrix-assisted laser desorption mass spectrometry (MALDI-MS) was performed at the MALDI-TOF facility of the Wistar Institute of the University of Pennsylvania.

Column chromatography was carried out on alumina (Aldrich, activated, neutral, Brockmann I, standard grade,  $\sim 150$  mesh, 58 Å) and on silica gel (Merck, 230–400 mesh, 60 Å). GPC was carried out on Biorad Biobeads S-X1 (mobile phase: THF) and Sephadex G-50 (mobile phase:  $H_2O$ ). All reagents were purchased from Sigma-Aldrich, Inc., Lancaster Synthesis, Inc., and Acros Organics, Inc. Solvents were purchased from Fisher Scientific, Inc., and purified using standard methods.

Analysis of spectroscopic data was performed using Origin 6.0, Microcal, Inc., software. The optimizations of dendrimer structures and molecular dynamics simulations were done on a 2.5 GHz PC workstation using Hyperchem 5.0 (Hypercube, Inc.) software. MM+ force field, as implemented in Hyperchem, was used in both optimizations and dynamics calculations. The calculation of electrostatic potential maps was done using GRASP software<sup>30</sup> on an SGI workstation. Poisson–Boltzmann solver, as implemented in GRASP, was used to build the electrostatic potential maps.

**UV–Vis and Fluorescence Measurements.** To obtain a series of samples for pH titrations, a small amount of porphyrin was dissolved in 75–100 mL of 50 mM  $K_2HPO_4$  solution and pH was adjusted by additions of KOH or HCl. The absorbance of the solution (1 cm cuvette) at a maximum of the porphyrin Soret band was kept below 1.5 OD for spectrophotometric determination ( $pK_{abs}$ ) or at about 0.1–0.15 OD for fluorescence measurements ( $pK_{flu}$ ). A small aliquot ( $\sim 2$ –3 mL) of the solution was transferred into a quartz cuvette, and the spectra were recorded. Normally, two titrations were performed to establish the

(35) Harold, F. M.; Baarda, J. R. *J. Bacteriol.* **1967**, *94*, 53.

(36) Urry, D. W.; Goodall, M. C.; Glickson, J. D.; Mayers, D. F. *Proc. Natl. Acad. Sci. U.S.A.* **1971**, *68*, 1907.

reversibility, e.g. beginning at basic pH down to acidic and backward. The ratio of the absorption intensities at two Soret peaks (free base vs dication) or a ratio of a Soret peak vs the isobestic point was plotted against pH and fitted to the Hasselbach equation. The parameter  $n$  in the Hasselbach equation was allowed to change during the search (see the main text).

Simultaneous titrations involving porphyrin and tetrabenzoporphyrin dendrimers were done in much the same way, except that the concentrations of the compounds had to be adjusted to obtain similar fluorescent responses from **1** (H<sub>2</sub>P-Glu<sup>4</sup>OH) and **2** (H<sub>2</sub>TBP-Nw<sup>1</sup>OH). The latter dendrimer had to be present in the mixture in excess (3–4 times), because of its significantly lower fluorescence quantum yield and lower sensitivity of the detection system in the longer wavelength range.

Fluorescence quantum yields were measured by comparing the integrals of the corrected emission spectra of the samples with those of free-base *meso*-tetraphenylporphyrin (H<sub>2</sub>TPP) in deaerated benzene. The spectra were recorded using Hamamatsu R2658P detector, and in the case of tetrabenzoporphyrins scanning was done up to 1000 nm. The spectra were normalized by the optical density of the samples at the excitation wavelength, relative photon intensity of the source, and quantum efficiency of the detector throughout the entire emission range. The reported quantum yield for H<sub>2</sub>TPP in benzene is 11%.<sup>37</sup> The measurements involving the core porphyrins **1a** and **2a** were performed in deaerated CH<sub>2</sub>Cl<sub>2</sub> solutions.

**Liposome Preparation and Dye Inclusion Experiments.** Phospholipid vesicles containing dye **1** were prepared as follows. L- $\alpha$ -Phosphatidylcholine (200 mg) was dissolved in a mixture of 1 mL of CHCl<sub>3</sub> and 0.5 mL of methanol in a glass test tube with a conic bottom. The solution was evaporated under a flow of nitrogen from the tube, which was kept under continuous rotation, leaving a phospholipid film on the tube walls. A 2 mL volume of solution containing 10 mM K<sub>2</sub>HPO<sub>4</sub> (pH 7.0), 50 mM KCl, and porphyrin dendrimer **1** was added to the tube, and the resulting suspension was sonicated on an ice bath using a microtip in pulsed mode (4 × 60, output 4:40%, sonicator Vibracell, Sonic & Materials, Inc.). To remove the outside dye, the freshly prepared liposomes were passed through a column (i.d. 1 × 7 cm) packed with Sephadex G200 (6 cm layer) and an anion-exchange resin (QAE-Sephadex A50, Pharmacia) (1 cm layer) at the bottom of the column to trap any remaining dye. After purification, the concentration of the dye in the outside solution was negligibly low, as evident by fluorescence measurements of the supernatant after centrifugation of the liposome solution.

The Fluorolog-2 system with R928 PMT was used to measure fluorescence in the experiments involving liposomes. The measurements were conducted using a standard 1 cm quartz cuvette, equipped with a stirrer and a pH minielectrode. pH changes inside the vesicles after addition of small aliquots of acid or base were monitored using fluorescence right angle detection setup. Gramicidin (0.2  $\mu$ g/mL, final concentration) was added directly to the cuvette as the measurements progressed, from a stock solution in DMSO. The amount of DMSO added (5  $\mu$ L) did not affect the proton permeability of the liposomes.

**Synthesis of the Core Porphyrins.** Core porphyrin **1b** was synthesized as described previously.<sup>9</sup> The synthesis of core porphyrin **2b** (Scheme 2) generally followed the recently published method.<sup>28</sup> The first three steps of the reaction sequence, leading to pyrrole ester **i**, are described in detail in refs 28 and 38. In the reported below UV-vis data for the porphyrins, the intensities (shown in parentheses) are given relative to the strongest absorption in the spectrum, i.e., the Soret band, whose intensity was set to 1.0. The positions of the absorption bands of the porphyrins were found to be solvent dependent and in the case of the porphyrin dications also dependent on the concentration and type of the acid added.

**Pyrrole ii.** Pyrrole-ester **i** (1.3 g, 3.5 mmol) was dissolved in 35 mL of THF, Et<sub>3</sub>N (0.35 mL) was added, and the vessel was flushed

with hydrogen. Pearlman catalyst<sup>39</sup> was cautiously added, and the reaction mixture was stirred under hydrogen, until TLC (CH<sub>2</sub>Cl<sub>2</sub>–THF) showed no presence of the original pyrrole-ester **i**. The catalyst was filtered off, the solvent was removed under vacuum, and the resulting product was refluxed in ethylene glycol for 40 min. The mixture was poured onto crushed ice, brine was added to reduce the emulsion, and the product was extracted with CH<sub>2</sub>Cl<sub>2</sub> (4 × 50 mL). The organic phase was thoroughly washed with water (200 mL), then with brine, and then dried over Na<sub>2</sub>SO<sub>4</sub>, and the solvent was removed in a vacuum. The resulting material was purified on a short (i.d. 2 × 10 cm) silica gel column (eluent CH<sub>2</sub>Cl<sub>2</sub>–THF, 20:1). Yield of pyrrole **ii**: 0.73 g, 88%. <sup>1</sup>H NMR (CDCl<sub>3</sub>):  $\delta$  8.05 (broad s, 1H), 6.5 (d, 2H,  $J = 2.5$  Hz), 3.65 (s, 6H), 2.88–3.27 (m, 6H).

**Porphyrin iii.** Pyrrole **ii** (0.59 g, 2.5 mmol) was dissolved in 250 mL of CH<sub>2</sub>Cl<sub>2</sub> and 4-(methoxycarbonyl)benzaldehyde (0.44 g, 2.7 mmol) was added to the mixture. The mixture was kept under continuous stirring in the dark at rt (room temperature) under Ar. After 10 min, BF<sub>3</sub>·Et<sub>2</sub>O (0.071 g, 0.5 mmol) was added in one portion, and the mixture was left to react for 2 h. DDQ (0.63 g, 2.8 mmol) was added, and the mixture was left overnight. The resulting solution was washed with 10% aqueous Na<sub>2</sub>SO<sub>3</sub> (100 mL), then with 10% aqueous Na<sub>2</sub>CO<sub>3</sub> (100 mL), and finally with 5% aqueous HCl, after which it was dried over Na<sub>2</sub>SO<sub>4</sub>. The solvent was removed in a vacuum, and the remaining material was purified on a silica gel column (eluent: CH<sub>2</sub>Cl<sub>2</sub>–THF and then CH<sub>2</sub>Cl<sub>2</sub>–THF–AcOH). A bright green band was collected, and after removal of the solvent, the remaining solid was purified by repetitive precipitations from CH<sub>2</sub>Cl<sub>2</sub>–AcOH (10:1) mixture with hexane. Yield of porphyrin **iii**: 315 mg, 33%. <sup>1</sup>H NMR (free base, CDCl<sub>3</sub>):  $\delta$  8.52 (m, 8H), 8.19–8.37 (m, 8H), 4.1 (s, 12H), 2.4–4.0 (m, 48H), –2.4 (br s, 2H). MALDI,  $m/z$ : calcd, 1527.5; found, 1528.4. UV-vis,  $\lambda_{\max}$  nm: (free base; CH<sub>2</sub>Cl<sub>2</sub>–Et<sub>3</sub>N, 10:1) 445 (1.00), 539 (0.09), 611 (0.04), 675 (0.02); (dication; CH<sub>2</sub>Cl<sub>2</sub>–TFA, 10:1) 461 (1.00), 611 (0.05), 669 (0.09).

**Copper Porphyrin iv.** An excess of Cu(OAc)<sub>2</sub>·2H<sub>2</sub>O (110 mg, 0.5 mmol) was added to a solution of porphyrin **iii** (180 mg, 0.118 mmol) in CHCl<sub>3</sub>–MeOH (9:1), and the mixture was stirred at rt for 10–15 min. The conversion was monitored using UV-vis spectroscopy (solvent CHCl<sub>3</sub>–AcOH). The reaction was stopped when the Soret absorption of the porphyrin dication (460–470 nm) disappeared. The mixture was washed with 10% aqueous AcOH and then with 10% aqueous NaHCO<sub>3</sub> and water and dried over Na<sub>2</sub>SO<sub>4</sub>. The solvent was evaporated in a vacuum, and the remaining material was purified on a silica gel column, giving the product as a red amorphous solid. Yield of Cu-porphyrin **iv**: 182 mg, 97%. MALDI,  $m/z$ : calcd, 1589.1; found, 1587.6. UV-vis,  $\lambda_{\max}$  nm (CH<sub>2</sub>Cl<sub>2</sub>): 428 (1.00), 559 (0.12), 593 (0.09).

**Copper Tetrabenzoporphyrin v.** Porphyrin **iv** (180 mg, 0.10 mmol) was dissolved in 50 mL of dry MeCN. DDQ (0.36 g, 1.6 mmol) was added, and the mixture was refluxed for 30 min. The color of the solution changed from reddish to bright green. The mixture was allowed to cool, diluted with CH<sub>2</sub>Cl<sub>2</sub>, washed with 10% aqueous Na<sub>2</sub>SO<sub>3</sub> solution and then with water and brine, and dried over Na<sub>2</sub>SO<sub>4</sub>. The solvent was removed in a vacuum, and the remaining solid was purified on a silica gel column (eluent CH<sub>2</sub>Cl<sub>2</sub>–THF, 10:1). The first dark-green fraction was collected. The solvent was evaporated, and the remaining material was recrystallized from CH<sub>2</sub>Cl<sub>2</sub>–ether to give the product as a blue-green crystalline solid. Yield of Cu-tetrabenzoporphyrin **v**: 169 mg, 95%. MALDI,  $m/z$ : calcd, 1572.9; found, 1572.8. UV-vis,  $\lambda_{\max}$  nm (CH<sub>2</sub>Cl<sub>2</sub>): 471 (1.00), 613 (0.11), 662 (0.35).

**Tetrabenzoporphyrin Ester 2a.** Compound **v** (150 mg, 0.095 mmol) was dissolved in 15–30 mL of concentrated H<sub>2</sub>SO<sub>4</sub> and left under stirring at rt for 24 h. The conversion was monitored using UV-vis spectroscopy (solvent: HCl concentrated), as the Soret band of **2a** dication emerged at 510–520 nm, while the Soret band of Cu-tetrabenzoporphyrin **v** disappear. The solution in H<sub>2</sub>SO<sub>4</sub> was carefully poured into ice-cold MeOH (100 mL, ice bath) and left in a closed vessel overnight. CH<sub>2</sub>Cl<sub>2</sub> (100 mL) and water (300 mL) were added to

(37) Seybold, P. G.; Gouterman, M. *J. Mol. Spectrosc.* **1969**, *31*, 1.

(38) (a) Haake, G.; Struve, D.; Montforts, F. P. *Tetrahedron Lett.* **1994**, *35*, 9703. (b) Abel, Y.; Haake, E.; Haake, G.; Schmidt, W.; Struve, D.; Walter, A.; Montforts, F. P. *Helv. Chim. Acta* **1998**, *81*, 1978. (c) Hopkins, P. B.; Fush, P. L. *J. Org. Chem.* **1978**, *43*, 1208.

(39) Perlman, W. M. *Tetrahedron Lett.* **1967**, *17*, 1663.

the resulting mixture. The organic layer was separated, washed with 10% aqueous  $\text{Na}_2\text{CO}_3$  solution and then with water, and dried over  $\text{Na}_2\text{SO}_4$ . The solvent was removed in a vacuum, and the remaining green solid was purified on a short silica gel column (i.d.  $2 \times 10$  cm, eluent  $\text{CHCl}_3$ –THF, 20:1). The major bright-green fraction was collected and evaporated to dryness, and the residual material was recrystallized from  $\text{CH}_2\text{Cl}_2$ –ether mixture. Yield of **2a**: 137 mg, 95%, blue-green crystals.  $^1\text{H}$  NMR ( $\text{CDCl}_3$ –TFA):  $\delta$  11.06 (TFA + NH), 8.68 (br, 16H), 7.77 (s, 8H), 4.24 (s, 12H), 3.83 (s, 24H).  $^{13}\text{C}$  NMR ( $\text{CDCl}_3$ –TFA):  $\delta$  166.8, 166.7, 141.3, 141.3, 136.0, 132.9, 132.8, 131.5, 131.2, 125.7, 116.1, 53.2, 53.1. MALDI-TOF,  $m/z$ : calcd, 1511.4; found, 1511.5. (UV–vis: see Table 1.)

**Tetrabenzoporphyrin Acid 2b.** Tetrabenzoporphyrin **2a** (100 mg, 0.066 mmol) was stirred overnight at rt with 0.5 g of LiOH in 20 mL of THF. Water (about 10 mL) was added, and THF was removed on a rotary evaporator under reduced pressure. The resulting deep green solution was filtered, and porphyrin **2b** was precipitated upon acidification with HCl. The precipitate was collected by centrifugation and dried in a vacuum. Yield of **2b**: 86 mg, 97%.  $^1\text{H}$  NMR (DMSO- $d_6$ –TFA):  $\delta$  8.77–8.55 (m, AA'BB'Ar, 16H), 7.52 (s, 8H).  $^{13}\text{C}$  NMR (DMSO- $d_6$ –TFA):  $\delta$  167.3, 166.7, 142.5, 141.8, 135.7, 132.2, 131.9, 123.8, 116.4. (UV–vis: see Table 2.)

**Synthesis of Porphyrin Dendrimers.** All carboxyl-terminated porphyrin dendrimers were obtained by hydrolysis of the corresponding esters. The procedures for hydrolysis and isolation by either precipitation or dialysis/liophilization were described in the earlier papers.<sup>9</sup> Gen 4 polyglutamic porphyrin dendrimer ethyl ester ( $\text{H}_2\text{P-Glu}^4\text{OEt}$ ) was synthesized divergently (see below) from its precursor Gen 3 dendrimer  $\text{H}_2\text{P-Glu}^3\text{OH}$ , which was in turn was synthesized from Gen 2 dendrimer ( $\text{H}_2\text{PorphGlu}^2\text{OH}$ ), according to the previously reported method.<sup>9c</sup> Gen 2 porphyrin dendrimer was synthesized by coupling Gen 2 triglutamic dendrons to the core porphyrin **1b**. Synthesis of Gen 2 dendron followed the earlier published method.<sup>9d</sup> Esterification of  $\text{H}_2\text{P-Glu}^2\text{OH}$  with monomethoxypoly(ethylene glycol) followed the reported protocol.<sup>7b,e,9d</sup> Gen 1 Newkome dendron was prepared as described earlier.<sup>29</sup> Solutions of all light-sensitive compounds were shielded from the ambient light during the syntheses. The UV–vis spectra of all intermediate porphyrin dendrimers were identical to those of the core porphyrins and/or of the compounds **1** and **2**, whose spectra are tabulated (Table 2) and described in the main text in great detail.

**$\text{H}_2\text{P-Glu}^2\text{OEt}$ .** Porphyrin **1b** (200 mg, 0.25 mmol) and 6 equiv of Gen 2 triglutamic dendron (0.78 g, 1.5 mmol) were dissolved in 50 mL of DMF under Ar. 1,3-Dicyclohexylcarbodiimide (DCC) (0.32 g, 1.55 mmol) and pyridine (2 mL) were added, and the mixture was stirred at rt for 3 days. The solvent was evaporated under vacuum at rt, and the remaining brown-purple residue was redissolved in  $\text{CH}_2\text{-Cl}_2$ . The white crystalline precipitate (dicyclohexylurea) was filtered off, and the product was purified by chromatography on silica gel using 4:1  $\text{CH}_2\text{Cl}_2$ –THF as a mobile phase, followed by preparative GPC on S-X1 beads. Yield: 0.52 g, 75%.  $^1\text{H}$  NMR ( $\text{CDCl}_3$ ):  $\delta$  8.74 (s, 8H), 8.42–7.20 (m AA'BB'Ar and NH, 28H), 4.88–4.74 (m, 12H), 4.40–4.20 (m, 32H), 2.80–2.25 (m, 48H), 1.75–1.50 (m, 48H), –2.92 (s, 2H).  $^{13}\text{C}$  NMR (DMSO- $d_6$ ):  $\delta$  173.6, 173.4, 172.0, 171.6, 166.4, 147.7, 143.9, 141.2, 135.2, 132.0, 127.1, 120.2, 66.1 (bs), 52.1 (bs), 31.9, 30.5 (bs), 30.1, 26.4 (bs). MALDI-TOF,  $m/z$ : calcd, 2788; found, 2789.

**$\text{H}_2\text{P-Glu}^2\text{OPEG350}$ .**  $\text{H}_2\text{P-Glu}^2\text{OH}$  (50 mg, 0.021 mmol), DCC (0.15 g, 0.7 mmol), hydroxybenzotriazole (BtOH) (0.1 g, 0.7 mmol), 3 mL of poly(ethylene glycol) monomethyl ether (average MW 350), and a drop of *sym*-collidine were stirred together at rt for 7 days. Ice-cold water (20 mL) was added, and the mixture was acidified with a drop of HCl and left in the dark at 4 °C overnight. White precipitate was filtered off, and pH of the solution was adjusted to neutral. The solution was filtered again on a nitrocellulose 0.25  $\mu\text{m}$  filter, and the product was isolated by GPC on Sephadex G50 using water as the mobile phase. The solution was liophilized, and the remaining viscous purple oil was redissolved in 3 mL of THF and re-purified by GPC on S-X1 column. Yield: 145 mg, 92%.  $^1\text{H}$  NMR ( $\text{CDCl}_3$ ):  $\delta$  8.76 (bs, 8H), 8.21–8.19 (m, 16H), 7.65–7.50 (m, 12H<sub>NH</sub>), 4.63 (32H, m), 4.29 (4H, m), 4.19

(8H, m), 3.58 (32H<sub>PEG350</sub>, m), 3.35 (~508H<sub>PEG350</sub>, m), 2.60–2.14 (8H, m).  $^{13}\text{C}$  NMR ( $\text{CDCl}_3$ ):  $\delta$  172.5, 171.2, 145.1, 141.3, 134.1, 133.4, 131.1, 125.8, 120.9, 71.9, 70.6 (bs), 69.0 (bs), 64.5, 63.8, 58.9, 53.0, 52.0, 30.5, 30.3, 26.95. MALDI-TOF,  $m/z$ : calcd (for average MW) 7650; found, 7600 (broad peak).

**$\text{H}_2\text{P-Glu}^4\text{OH}$  (1).**  $\text{H}_2\text{P-Glu}^3\text{OH}$  (1.11 g, 0.25 mmol), glutamic acid diethyl ester hydrochloride (3.83 g, 16 mmol), DCC (3.3 g, 16 mmol), 18-crown-6 polyether (0.3 g, 1.1 mmol), and pyridine (2 mL) were left to react in 50 mL of DMF under Ar at 45 °C for 21 days. During the reaction, the solution slowly turned purple, indicating gradual extraction of porphyrin into the liquid phase. The solvent was evaporated under vacuum on a rotary evaporator, and the remaining brown material was redissolved in  $\text{CH}_2\text{Cl}_2$ . Dicyclohexylurea was filtered off, and the product was purified by chromatography on silica gel using 2:1  $\text{CH}_2\text{Cl}_2$ –THF as a mobile phase, followed by GPC on S-X1 beads. Yield of  $\text{H}_2\text{P-Glu}^4\text{OEt}$ : 0.95 g, 37%. MALDI-TOF,  $m/z$ : calcd, 10 326; found, 10 349 [(M + Na<sup>+</sup>) + satellites] (see the main text for details).  $\text{H}_2\text{P-Glu}^4\text{OEt}$  was hydrolyzed under basic conditions as described previously.<sup>9</sup> Porphyrin dendrimer **1** was purified by dialysis and isolated as a fluffy green powder after lyophilization.  $^1\text{H}$  NMR:  $\delta$  9.12 (bs, 8H), 8.51–8.42 (m, 16H), 4.76–4.20 (m, 60H), 2.80–1.8 (m, 240H).  $^{13}\text{C}$  NMR ( $\text{D}_2\text{O}$ ):  $\delta$  181.95, 181.9, 179.6, 176.0, 146.6, 142.7, 136.4, 127.9, 122.3, 112.9, 56.4, 55.0, 54.2, 35.3, 34.8, 34.6, 33.2, 32.9, 29.6, 29.0, 28.9, 28.6, 25.8, 25.3. In the  $^{13}\text{C}$  NMR spectrum of **1** the peaks in the glutamate region (60–20 ppm) consist of multiple resonances and therefore appear as broadened.

**$\text{H}_2\text{TBP-Nw}^1\text{OMe}$  (2c).** Tetrabenzoporphyrin **2b** (89 mg, 0.066 mmol), 24 equiv of Newkome dendron (0.6 g, 1.58 mmol), and BtOH (0.21 g, 1.58 mmol) were dissolved in 50 mL of DMF under Ar at 0 °C. DCC (0.32 g, 1.58 mmol) and 0.1 mL of *sym*-collidine were added, and the mixture was allowed to gradually warm to rt, after which it was stirred continuously for 3 days. The solvent was removed under vacuum, and the product was purified twice by GPC on S-X1 beads. Yield: 303 mg, 81%.  $^1\text{H}$  NMR ( $\text{CDCl}_3$ ):  $\delta$  8.39–8.32 (AA'BB'Ar, 16H), 7.30 (bs, 8H), 7.12 (s, 4H), 6.49 (s, 8H), 4.01 (s, 24H), 3.83 (t, 24H), 3.75–3.70 (m, 96H), 3.69 (s, 36H), 3.50 (s, 72H), 2.67 (t, 24H), 2.57 (t, 48H).  $^{13}\text{C}$  NMR ( $\text{CDCl}_3$ ):  $\delta$  172.0, 171.9, 168.5, 166.2, 146.8, 142.8, 139.1, 136.4, 134.6, 128.2, 123.9, 121.9, 116.1, 69.6, 69.0, 66.9, 66.7, 60.5, 60.2, 51.6, 51.5, 51.4, 51.3, 34.8. MALDI-TOF,  $m/z$ : calcd, 5679; found, 5702 (M<sup>+</sup> + Na), 5680 (M<sup>+</sup>), 5343 (see the main text for details).

**$\text{H}_2\text{TBP-Nw}^1\text{OH}$  (2).** Excess of NaOH (0.5 g) was added to a solution of **2c** (200 mg, 0.035 mmol) in 10 mL of THF. The mixture was stirred at rt for 4 h, and the solvent was evaporated under vacuum at rt. Water was added to the remaining solid, and the mixture was stirred at rt for additional 2 h. The solution was neutralized by HCl, filtered, dialyzed against distilled water for 4 days, and lyophilized.  $^1\text{H}$  NMR ( $\text{D}_2\text{O}$ ):  $\delta$  9.14–8.44 (m, 16H), 7.44 (bs, 8H), 9.5–7.0 (bm, 12H<sub>NH</sub>), 3.75 (bm, 144H), 2.71 (bm, 72H).  $^{13}\text{C}$  NMR ( $\text{D}_2\text{O}$ ): 178.8, 178.4, 178.1, 177.9, 171.5, 171.3, 169.3, 143.6, 142.7, 137.9, 137.1, 136.0, 129.8, 125.6, 125.5, 118.2, 115.8, 70.7, 70.3, 69.0, 68.8, 62.8, 62.4, 36.8, 36.6.

**Acknowledgment.** The Grant NS-31465 from the NIH (U.S.), the Contract No. 02-5403-21-2 with Anteon Corp. (U.S.), and a grant from Carl Tryggers Foundation (Sweden) are gratefully acknowledged. C.H. and S.V. acknowledge The Royal Physiographic Society (Lund, Sweden) for the support of the international collaboration. A.G. acknowledges the postdoctoral scholarship from the Wenner-Gren Foundation (Sweden). We thank Prof. David F. Wilson for many invaluable discussions, Prof. Kim Sharp and Dr. Ninad Prahu for assistance with GRASP software, and Ms. Natalie Kim for proofreading the manuscript.

JA0341687